The use of force-volume microscopy to examine bacterial attachment to titanium surfaces

Chongzheng Na · Christopher J. McNamara ·
Nick R. Konkol · Kristen A. Bearce · Ralph Mitchell ·
Scot T. Martin

Abstract Force-volume microscopy (FVM) was used to study the interfacial and adhesive forces affecting primary bacterial attachment to surfaces. Forces were measured for titanium surfaces immersed either in cation-enriched (CE) solutions of yeast extract amended with phosphate buffer or in control solutions lacking the cation enrichment. The FVM measurements demonstrated that regions of elevated interfacial repulsion covered $72(\pm 2)\%$ of the surfaces immersed in CE solutions, compared to $26(\pm 2)\%$ for immersion in control solutions. Parallel collection of scanning electron micrographs demonstrated that surface densities of attached *Pseudomonas aeruginosa* were approximately $0.62(\pm 1.3)\times 10^6$ cells cm^{-2} compared to $8.7(\pm 0.8)\times 10^6$ cells cm^{-2} for surfaces immersed in the CE and control solutions, respectively. Interfacial repulsion indicated by FVM measurements therefore served as a predictor of bacterial attachment. Another factor influencing bacterial attachment was the adhesion force. FVM measurements indicated that the upper fifth percentile of surface adhesion was $1784(\pm 40)$ pN for surfaces immersed in the CE solution compared to $2284(\pm 40)$ pN for the control solutions. The more extensive regions of elevated interfacial repulsion as well as of decreased surface adhesion provide an explanation for the lower density of attached cells observed for the surfaces immersed in the CE compared to the control solutions. The conclusion is that FVM is a sensitive and informative technique that can be used to measure and explain interactions between microorganisms and surfaces.

Keywords Force-volume microscopy · Atomic force microscopy · *Pseudomonas aeruginosa* · Interfacial forces · Surface adhesion

C. Na · C. J. McNamara · N. R. Konkol · K. A. Bearce ·
R. Mitchell · S. T. Martin (✉)
School of Engineering and Applied Sciences, Harvard University,
29 Oxford Street,
Cambridge, MA 02138, USA
e-mail: scot_martin@harvard.edu
URL: http://www.seas.harvard.edu/environmental-chemistry

C. J. McNamara
School of Public Health, Harvard University,
Cambridge, MA, USA

S. T. Martin
Department of Earth and Planetary Sciences, Harvard University,
Cambridge, MA, USA

Present Address:
C. Na
Department of Civil Engineering and Geological Sciences,
University of Notre Dame,
Notre Dame, IN 46556, USA

Introduction

Many bacteria survive and grow in natural and engineered environments by attaching to surfaces (Hall-Stoodley et al. 2004). Surface-attached bacterial cells may develop into biofilms, which can have both beneficial and adverse effects on public health and engineering practices. Attached bacteria can help degrade recalcitrant pollutants in drinking water, wastewater, and groundwater (Singh et al. 2006; Bayless and Andrews 2008; Simpson 2008). They are, however, also responsible for metal corrosion, bacterial infection, and water-quality deterioration (Costerton et al.

1999; Szewzyk et al. 2000; Parsek and Fuqua 2004; Berry et al. 2006; September et al. 2007).

The initial stage of biofilm formation, which is bacterial attachment, is regulated in part by (1) the physical and chemical surface properties that influence distant interfacial forces prior to attachment, and (2) the adhesive forces after attachment (Marshall et al. 1971; Bos et al. 1999). When bacteria approach a surface, they encounter interfacial repulsion of electrostatic or steric origins. The bacteria must overcome this repulsion via Brownian motion, gravitation, diffusion, convection, cell motility, or their own pili. Once bacteria establish contact with a surface, they must resist hydraulic shear forces to remain attached. Successful surface adhesion is attributable to a combination of van der Waals attraction and chemical bonding.

The interfacial and adhesive forces that characterize bacterial–surface interactions can be measured with force-volume microscopy (FVM). FVM is a derivative of atomic force microscopy (AFM), which uses a miniature probe to survey a surface in a raster fashion. At each sample location, FVM sets the probe initially more than 100 nm away from the surface and then gradually reduces the probe–surface distance while the interfacial force is measured. After contact with the surface, the probe is slowly pulled away and the surface adhesion is measured before the probe–surface contact is broken. This description of FVM represents an analogy to the physicochemical model of bacterial attachment.

Previous applications of FVM to the study of bacterial attachment are limited mostly to surface adhesion (Abu-Lail and Camesano 2003a; Salerno et al. 2004; Vadillo-Rodriguez and Logan 2006; Sheng et al. 2007; Ma et al. 2008). In comparison, in this study we used FVM to simultaneously measure the interfacial force and the surface adhesion while varying solution chemistry. We correlated the interfacial force and the surface adhesion to the surface densities of attached bacteria. Solution chemistry was varied between a control solution and a solution enriched in multivalent cations, which are known to affect bacterial attachment. The study was carried out on a model system of medical and engineering significance, consisting of a titanium surface colonized by *Pseudomonas aeruginosa* (PAO1). Titanium is commonly used to make medical and dental implants, where bacterial attachment can cause infection (Montanaro et al. 2007). Titanium is also used to build heat exchangers used for desalination, where biofilm formation can dramatically reduce the heat transfer efficiency and increase operational cost (Characklis 1981). *Pseudomonas aeruginosa* is an opportunistic pathogen that is ubiquitous in the environment and is widely used in studies of biofilm formation (Costerton et al. 1999; An et al. 2006).

Materials and methods

Experimental procedures

Titanium coupons (Goodfellow Cambridge; Huntington, UK; surface area of 0.5×0.5 cm^2; thickness of 0.5 mm; composition: 90% Ti, 6% Al, 4% V) were sanitized with 80% ethanol and washed with deionized (DI) water. The coupons were placed in multiple 225-mL flasks, and 50 mL of either control or cation-enriched (CE) solution was added to a flask. The control solution was prepared by dissolving 0.22 g $(NH_4)_2SO_4$, 0.12 g KH_2PO_4, 0.23 g $MgSO_4 \cdot 7H_2O$, 0.25 g $CaCl_2 \cdot 2H_2O$, and 0.05 g BBL™ yeast extract (Becton Dickinson, Sparks, MD) in 1,000 mL water, followed by autoclave sterilization. The CE solution was prepared as described for the control but with water first equilibrated with four ferrous ferric chloride (FFC) ceramic balls (Akatsuka Group, Tsu-City, Japan) under vigorous stirring for 1 h. Both the CE and control solutions had a pH of 4.7. Further characterization of the solution chemistry is provided in Table S1.

One-half of the prepared flasks of each type ($n=3$) were inoculated with *P. aeruginosa*. Coupons immersed in the *P. aeruginosa*-inoculated solutions were removed after 4 days of incubation at 25°C and 120 rpm. The density of attached cells was then examined by scanning electron microscopy (SEM). The second half of the prepared flasks of each type (i.e., CE and control solutions without *P. aeruginosa* innoculation) remained sterile. The coupons in these flasks were examined by FVM following 2 days of immersion and shaking. Monitoring the change of surface forces over a 4-day period was technically difficult. Therefore, a representative sampling point was selected for force measurement in the middle of the attachment experiment.

For SEM analysis, titanium coupons removed from the flasks were washed and dehydrated in a series of ethanol solutions (40, 50, 60, 70, 80, 90, 95 and 100% ethanol). After dehydration, samples were critical-point dried (Autosamdri-815, Tousimis, Rockville, MD) and gold or palladium sputter-coated (Hummer II Sputter Coater, Anatech, Springfield, VA). Scanning electron micrographs of *P. aeruginosa* adhered to the surface were obtained with a Supra™ 55VP scanning electron microscope (Zeiss, Oberkochen, Germany) at an operating voltage of 2 kV.

P. aeruginosa cells adhered to the titanium surface were enumerated using two methods. First, cells were counted in SEM images based on size and shape. Attached bacteria were also enumerated by staining with 4′,6-diamidino-2-phenylindole (DAPI). Titanium coupons were rinsed gently with sterile deionized water and placed in sterile centrifuge tubes of 0.18% NaCl. Coupons were sonicated for 5 min in

a water bath sonicator (Branson 2510, Danbury, CT), after which the NaCl solution was filtered onto black polycarbonate filters. Bacteria were stained with DAPI and enumerated using epifluorescence microscopy.

For the FVM measurements, coupons removed from each type of flask were fixed onto a steel puck by dental wax. The coupon–puck assembly was sealed inside a fluid cell at 25($\pm$2)°C, which was then filled by syringe with sterile immersion solution; 100 fluid-cell volumes of solution were passed prior to the FVM measurements. Because the same immersion solution was used in washing, the adsorbed organic polymer layer was preserved.

Atomic force microscopy and force-volume microscopy

The topography, long-distance interfacial forces, and adhesive properties of the solution–coupon combinations were examined using a Veeco multimode scanning probe microscope. The microscope was equipped with a NanoScope IIIa controller, a signal access module, and a 50-μL fluid cell. Silicon-nitride probes (model: NP-S) were used. AFM and FVM are standard modes of operation included in the Veeco software (version 4.43r8) and hardware. Contact-mode AFM was first used to locate a representative area of 3×3 μm^2. FVM was then conducted with a lateral resolution of 32×32 sampling locations (i.e., 94×94 nm^2 per sampling point). Force measurements were performed after the detector output stabilized, indicating thermal equilibrium (Wenzler et al. 1996).

The principles of FVM are documented in the literature (Butt et al. 2005), and we described our implementation recently (Na and Martin 2008). In brief, FVM scans a representative area in a raster fashion. At each sampling location, a force-distance curve is recorded. The probe starts ca. 125 nm above the surface and gradually approaches in steps of less than 0.5 nm. At each step, the cantilever deflection d measured by the laser probe is related to interfacial and surface forces f through Hook's law: $f = kd$, where k is the cantilever spring constant. By convention, f is positive for repulsion and negative for attraction.

Results

Figure 1 shows representative SEM images of titanium surfaces previously immersed in the cation-enriched or control solutions. Comparison of Fig. 1a and b shows that the surface immersed in the CE solution has a lower density of attached *P. aeruginosa* cells ($6.2 \pm 1.3 \times 10^5$ cells cm^{-2}) than the surface immersed in the control solution ($8.7 \pm 0.8 \times 10^6$ cells cm^{-2}). Analysis by epifluorescence

microscopy gives similar rank ordering (CE: $3.9 \pm 0.5 \times 10^4$ cells cm^{-2}; control: $8.4 \pm 2.3 \times 10^4$ cells cm^{-2}).

Figure 2 shows representative force-distance curves at one location (i.e., one element of a FVM raster scan) for a surface immersed in the sterile CE solution. An approaching curve (Fig. 2a) and a retracting curve (Fig. 2b) are shown. The FVM results are not affected by surface roughness because every force-distance curve is measured from the same height, specifically 135 nm above the surface (i.e., topographical differences are corrected among sample locations).

In Fig. 2a, the probe approaches the surface from +125 nm, remains uninfluenced until approximately +50 nm, and experiences a repulsive force for +50 to +7 nm. Attractive forces begin at closer distances and exceed the repulsive forces for +6.2 nm and closer. At +5.3 nm, the probe establishes physical contact with organic polymers from the yeast extract in the solution (i.e., those adsorbed on the titanium surface). Pressing the probe further deforms the polymer layer, as illustrated by the force-distance relation from +5.3 to +0.0 nm. In contrast, for surfaces immersed in solutions without yeast, there is no polymer layer and this region is absent (data not shown). Where the probe and the surface are physically separate (i.e., from +125 to +5.3 nm), a maximum value of interfacial repulsion of 118 pN ($f_{rep,max}$) occurs at $z_{rep,max}$ of +10.4 nm (Fig. 2a).

In Fig. 2b, the force-distance response is shown as the probe pulls away from the surface. From +0.0 to +25 nm, the probe remains adhered to the polymer layer on the surface. As the pulling force increases, the polymer layer adjusts and remains in contact with the probe. Beyond +25 nm, the probe breaks free from the surface, snapping to +40 nm. Between +0.0 and +25 nm, a maximum value $f_{adh,max}$ in surface adhesion of −431 pN occurs at $z_{adh,max}$ of +18.9 nm (Fig 2b).

Figure 3 shows the topography and FVM images for surfaces immersed in the CE or control solutions. The image size of 3×3 μm^2 is comparable to the area occupied by a single cell on the control surface (Fig. 1b). Figure 3a,d shows that the surfaces immersed in the CE and control solutions have microscopically similar grooves of ca. 0.5 to 1 μm roughness. Figure 3b,c and e,f show that both $f_{rep,max}$ and $-f_{adh,max}$ are distributed randomly for surfaces immersed in both solutions. Furthermore, the mean values of the maximum interfacial repulsion in the two solutions (71$\pm$30 pN and 60$\pm$30 pN) are similar (Fig. 4a,b). Surfaces immersed in the two solutions differ, however, in the relative area having non-zero (i.e., positive) interfacial repulsion, with $\theta_{rep,max}$(positive)=72($\pm$2)% for the surfaces immersed in the CE solution and $\theta_{rep,max}$(positive) = 26($\pm$2)% for those in the control solution (Fig. 4a,b).

Analysis of the maximum surface adhesion is shown in Fig. 5. The density of attached cells has been shown in the

Fig. 1 Scanning electron microscopy (SEM) image of titanium surfaces immersed in **a** cation-enriched or **b** control solutions for 4 days. Prior to immersion SEM images showed clean surfaces. Image size: 40× 40 μm²
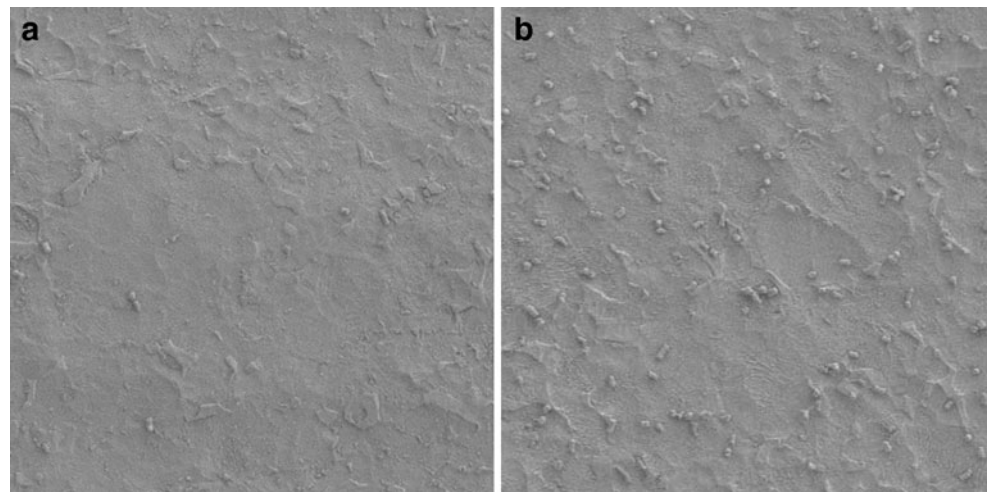

literature to correlate with the upper fifth percentile of surface-adhesion force (i.e., the 95% point of the cumulative distribution function of $-f_{adh,max}$) (17, 30). Figure 5 shows that $-f_{adh,max}$(95%) was lower for the CE treatment (1,784±40 pN) than for the control (2,284±40 pN).

The presence of a surface-adsorbed organic polymer layer is confirmed by the analysis of histograms of $z_{rep,max}$ and $z_{adh,max}$. Least-square Gaussian fits to the histograms of $z_{rep,max}$ identify four approximately equally spaced layers, which can be attributed to heterogeneity in the number of adsorbed layers of biopolymers across the surface sampled by the FVM scan (Fig. 6a,b). The average of the peak-to-peak differences represents the thickness of a biopolymer layer. The average biopolymer layer thickness is 5.0(±0.2) nm in the CE solution and 4.3(±0.5) nm in the control solution. Although the layers are less pronounced for

adhesion when the tip is retracted, four layers are still apparent (Fig. 6c,d). Based on the value of $z_{adh,max}$, the average biopolymer layer thickness is 6.2(±0.9) nm in the CE solution 5.1(±1.1) nm in the control solution. The difference between the layer thickness estimated from repulsive and adhesive forces can be explained by compression of the polymer layers for a descending probe and expansion of the polymer layers for a retracting probe.

Discussion

Figure 7 summarizes the results for surfaces immersed in the CE solution compared to those immersed in the control solution. The bacterial density on the coupons, the percent of the surface area having non-zero interfacial repulsion,
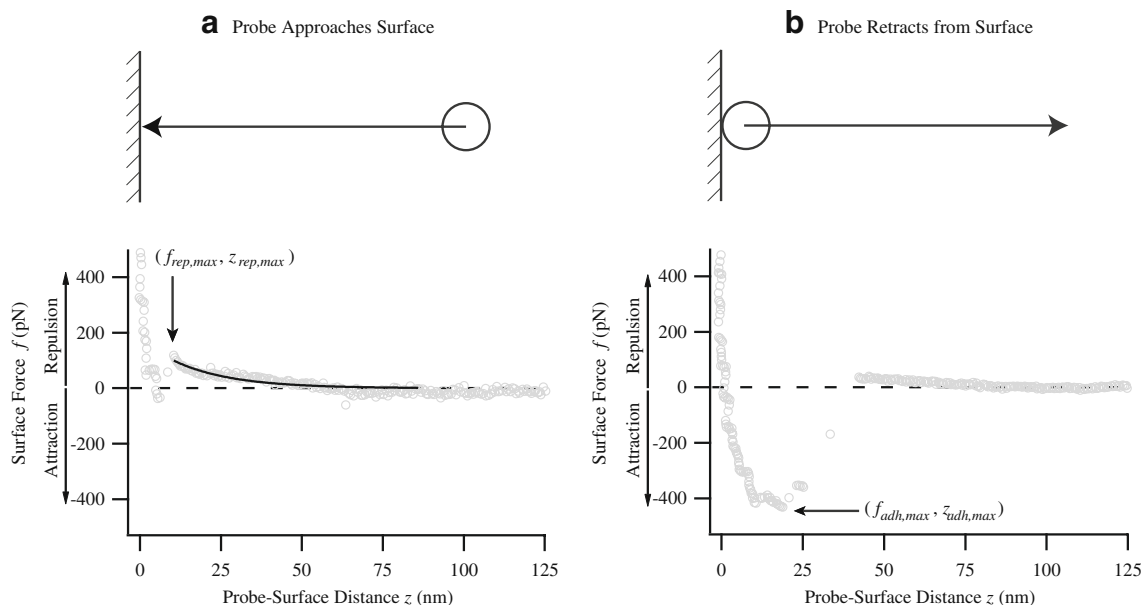

Fig. 2 Representative force-distance curves collected by force-volume microscopy (FVM) on a titanium surface immersed in sterile cation-enriched solution for 2 days. Curves are collected with the immersion solution still in place. *Arrows* show Positions of f_{max} and z_{max}

Topography   Maximum Interfacial Repulsion   Maximum Surface Adhesion
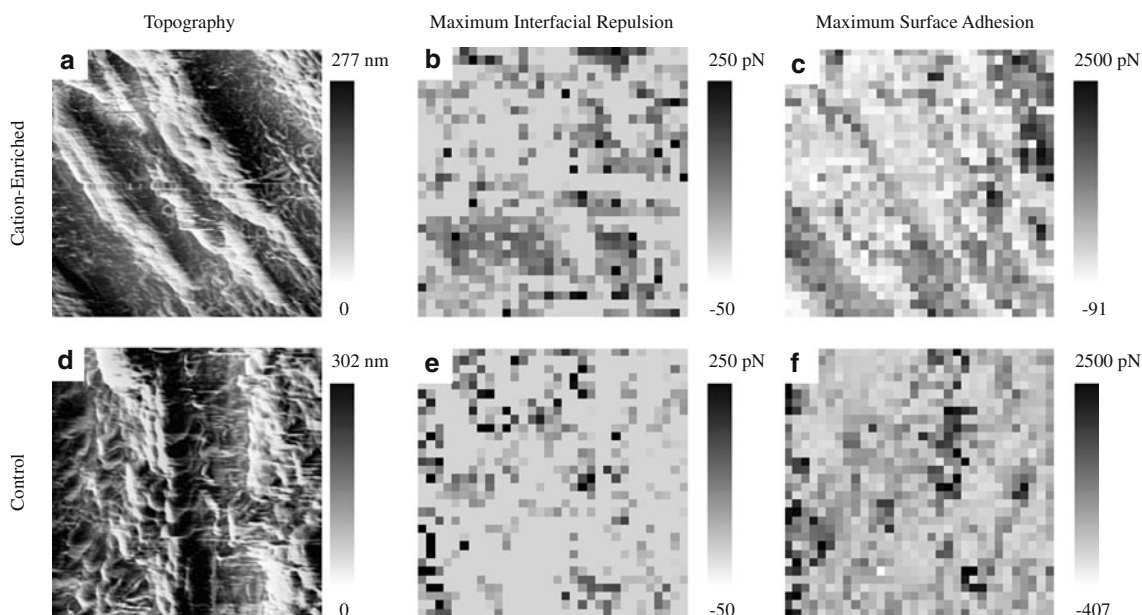
Fig. 3 False-color images collected by FVM of topography, maximum interfacial repulsion, and maximum surface adhesion for titanium surfaces immersed in **a**–**c** cation-enriched, or **d**–**f** control solutions for 2 days. The solutions were sterile. Images were collected in the immersion solution. Image size: 3×3 μm^2
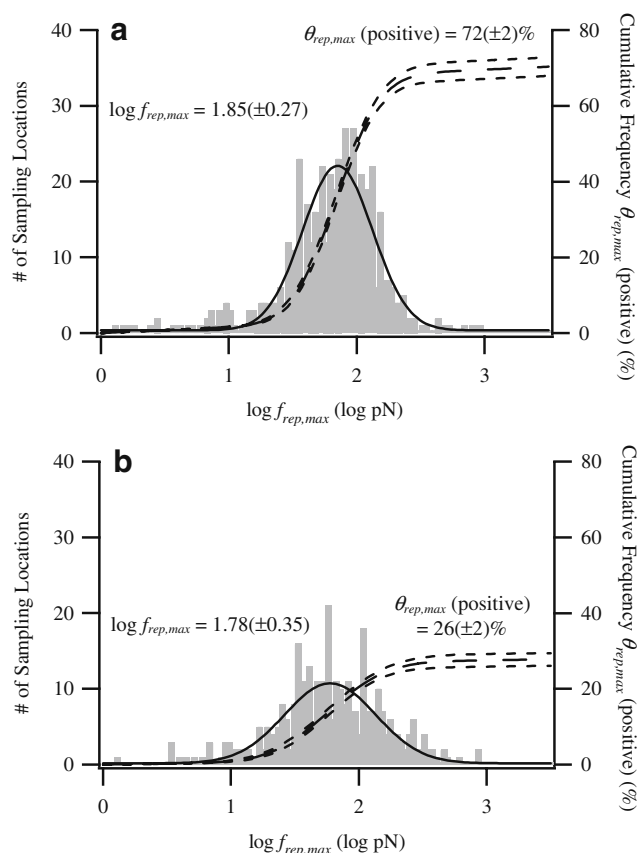

Fig. 4 Statistical analyses of images of maximum interfacial repulsion from Fig. 3 for **a** cation-enriched or **b** control solutions. *Solid curves* Gaussian fits. The *dashed* and *dotted curves* represent the means and standard errors of the cumulative frequencies, respectively, computed by normalizing to the total number of sampling locations on each surface
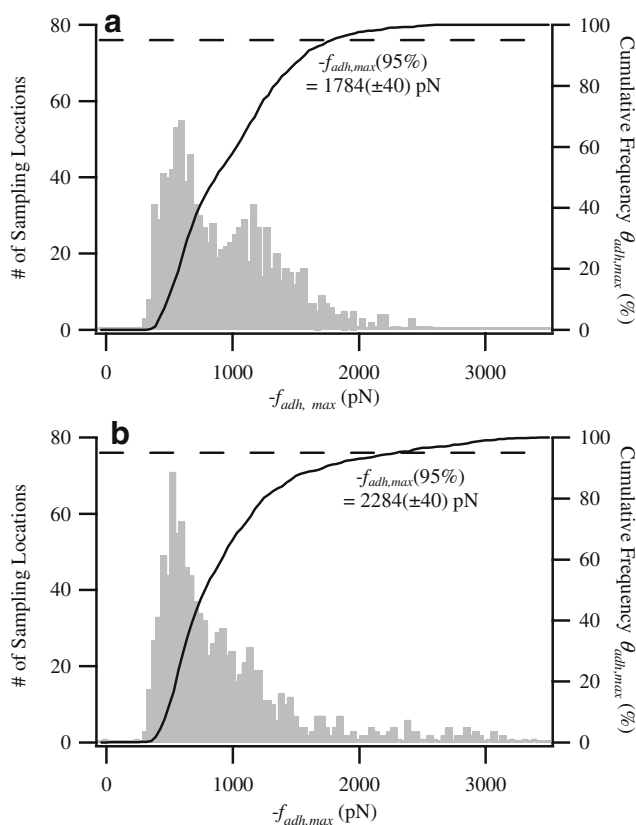
Fig. 5 Statistical analyses of the images of the maximum surface adhesion from Fig. 3 for **a** cation-enriched or **b** control solutions. *Solid curves* Cumulative frequencies, with standard errors of ca. 40 pN. *Dashed lines* 95% cumulative frequencies

Fig. 6 Histograms of probe–surface distances of **a**, **b** maximum interfacial repulsion, and **c**, **d** maximum surface adhesion
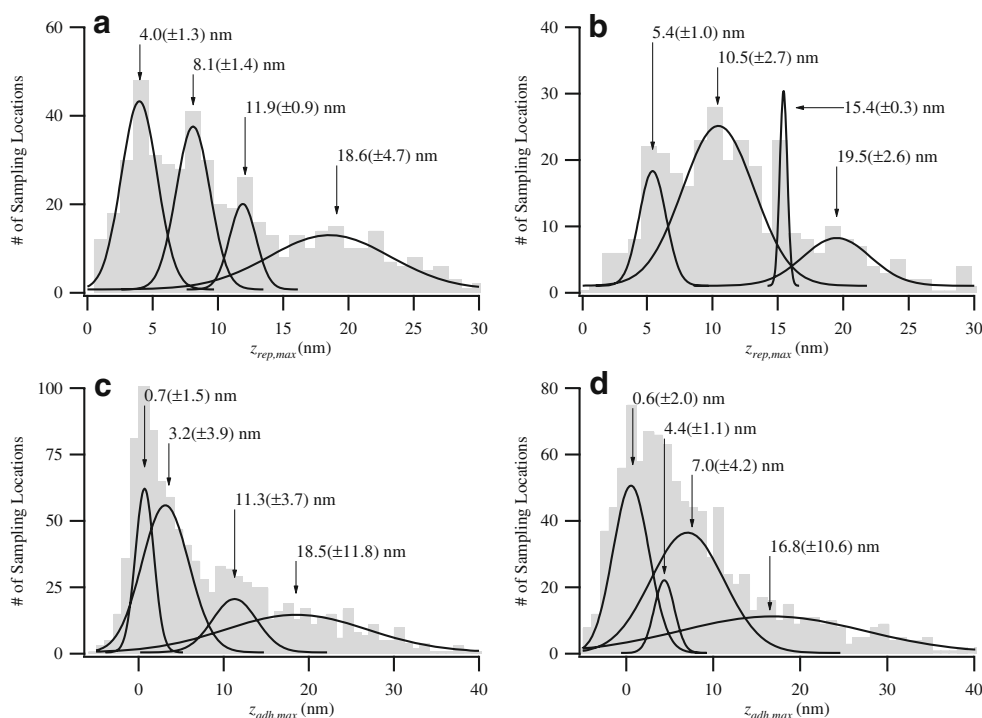
and the value of the 95th percentile of maximum surface adhesion are represented by the bar heights. The difference between bacterial densities for coupons immersed in the CE compared to those in the control solutions may be explained by the combined effects of the repulsive and adhesive forces. Greater repulsion and reduced adhesion both contribute to the explanation of why the surfaces immersed in the CE solution have decreased bacterial attachment compared to those immersed in the control solution. Bacterial cells attach less readily to the CE-treated surfaces, and the cells that do attach are more easily removed by hydraulic shearing forces.
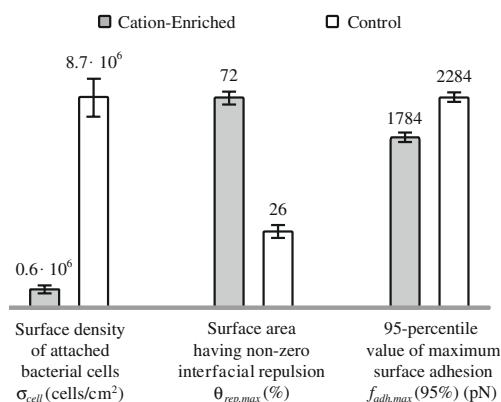
Fig. 7 Comparison for cation-enriched and control solutions of surface cell density, surface area having non-zero interfacial force, and the 95-percentile value of maximum surface adhesion. Surface cell density is based on analysis of SEM images

The organic polymers introduced by the yeast extract present in both solutions have a tendency to coat surfaces (Baty et al. 1996). The long-range characteristics of the interfacial repulsion from +50 to +5.3 apparent in Fig. 2a suggest a steric repulsion by outer layers of surface-adsorbed organic polymers (Heinz and Hoh 1999). Titanium surfaces, which are usually covered by an oxide layer (Sykes et al. 2002), adsorb biopolymers such as proteins and polysaccharides from aqueous solution. An alternative explanation of electrostatic repulsion for the results from +50 nm to +5.3 nm can be ruled out because the ionic strength of the solution is high enough (i.e., greater than 18 mM; cf. Table S1) that a Debye length κ^{-1} of under 3 nm is expected, screening out electrostatic forces at greater distances (Israelachvili 1991; Na and Martin 2008).

The observation that surfaces immersed in the CE solution have lower surface adhesion than those immersed in the control solution [i.e., $-f_{adh,max}(CE, 95\%) < -f_{adh,max}(control, 95\%)$] may be explained by enhanced compression in the polymer layers of the CE solution (Fig. 6). In addition to bridging between the functionalities on the organic polymers and those on the titanium surface, Ca^{2+} and Mg^{2+} also bridge one polymer to another. Thus, the higher concentration of multivalent cations in the CE solution results in a more compressed polymer layer. Abu-Lail and Camesano (2003b) similarly described compression of the polymer layer on bacterial surfaces at high ionic strength.

Compression of the biopolymer layer by Ca^{2+} and Mg^{2+} is also consistent with the observation that the average

polymer layer thickness was greater in the CE solution than in the control. Because the functionalities of the polymers in the compressed layer are bridging to one another, fewer contact sites are available for adhesion to the AFM probe. As a result, $-f_{\text{adh,max}}(95\%)$ in the control was greater than $-f_{\text{adh,max}}(95\%)$ in the CE treatment. Our observation that the surface area having non-zero interfacial repulsion was greater in the CE solution than in the control can likewise be explained by the presence of the multivalent cations Ca^{2+} and Mg^{2+}, as well as the anion phosphate (PO_4^{3-}), in the CE solution. These multivalent ions enhance organic polymer adsorption (Damen et al. 1991; Klinger et al. 1997).

The Derjaguin, Landau, Verwey and Overbeek (DVLO) theory, which has been used to interpret the initial steps of bacterial adhesion to surfaces, predicts a reduction in electrostatic and van der Waals forces that create a barrier for bacterial attachment as ionic strength increases (van Loosdrecht et al. 1989). DVLO predictions are borne out by studies showing that reductions in Ca^{2+} and Mg^{2+} concentration reduce bacterial attachment (Marshall et al. 1971). The presence of the organic polymer layer on the surface, however, alters the relationship between ionic strength and adhesion. Specific interactions between ions and polymer depend on characteristics of both the ionic solution and the polymer layer. For example, increasing concentrations of KCl produces a rigid polymer layer that interacts strongly with the AFM tip (Abu-Lail and Camesano 2003b). In contrast, the results of the present study show that Ca^{2+} and Mg^{2+} bind the polymer molecules and thereby reduce interactions with the AFM tip.

Bacterial attachment under some circumstances is facilitated by factors such as swimming motility, pili, and extracellular polysaccharides. The correlation between attached cell density and the FVM measurements suggests that bacterial attachment for our experimental system is mainly a physicochemical process (Bos et al. 1999; Marshall et al. 1971). Under these circumstances, an abiotic AFM tip can effectively represent a bacterial cell. FVM is a new and powerful tool that can be used to measure microbial interactions with surfaces.

References

Abu-Lail NI, Camesano TA (2003a) Role of lipopolysaccharides in the adhesion, retention, and transport of *Escherichia coli* JM109. Environ Sci Technol 37:2173–2183

Abu-Lail NI, Camesano TA (2003b) Role of ionic strength on the relationship of biopolymer conformation, DLVO contributions, and steric interactions to bioadhesion of *Pseudomonas putida* KT2442. Biomacromolecules 4:1000–1012

An D, Danhorn T, Fuqua C, Parsek MR (2006) Quorum sensing and motility mediate interactions between *Pseudomonas aeruginosa* and *Agrobacterium tumefaciens* in biofilm cocultures. Proc Natl Acad Sci USA 103:3828–3833

Baty AM, Frolund B, Geesey GG, Langille S, Quintero EJ, Suci PA, Weiner RM (1996) Adhesion of biofilms to inert surfaces: a molecular level approach directed at the marine environment. Biofouling 10:111–121

Bayless W, Andrews RC (2008) Biodegradation of six haloacetic acids in drinking water. J Water Health 6:15–22

Berry D, Xi CW, Raskin L (2006) Microbial ecology of drinking water distribution systems. Curr Opin Biotechnol 17:297–302

Bos R, van der Mei HC, Busscher HJ (1999) Physico-chemistry of initial microbial adhesive interactions—its mechanisms and methods for study. FEMS Microbiol Rev 23:179–230

Butt HJ, Cappella B, Kappl M (2005) Force measurements with the atomic force microscope: technique, interpretation and applications. Surf Sci Rep 59:1–152

Characklis WG (1981) Fouling biofilm development—a process analysis. Biotechnol Bioeng 23:1923–1960

Costerton JW, Stewart PS, Greenberg EP (1999) Bacterial biofilms: a common cause of persistent infections. Science 284:1318–1322

Damen JJM, Tencate JM, Ellingsen JE (1991) Induction of calcium-phosphate precipitation by titanium-dioxide. J Dent Res 70:1346–1349

Hall-Stoodley L, Costerton JW, Stoodley P (2004) Bacterial biofilms: from the natural environment to infectious diseases. Nat Rev Microbiol 2:95–108

Heinz WF, Hoh JH (1999) Spatially resolved force spectroscopy of biological surfaces using the atomic force microscope. Trends Biotechnol 17:143–150

Israelachvili JN (1991) Intermolecular and surface forces, 2nd edn. Academic, Boston

Klinger A, Steinberg D, Kohavi D, Sela MN (1997) Mechanism of adsorption of human albumin to titanium in vitro. J Biomed Mater Res 36:387–392

Ma H, Winslow CJ, Logan BE (2008) Spectral force analysis using atomic force microscopy reveals the importance of surface heterogeneity in bacterial and colloid adhesion to engineered surfaces. Colloids Surf B Biointerfaces 62:232–237

Marshall KC, Stout R, Mitchell R (1971) Mechanism of initial events in sorption of marine bacteria to surfaces. J Gen Microbiol 68:337–348

Montanaro L, Campoccia D, Arciola CR (2007) Advancements inmolecular epidemiology of implant infections and future perspectives. Biomaterials 28:5155–5168

Na CZ, Martin ST (2008) Interfacial forces are modified by the growth of surface nanostructures. Environ Sci Technol 42:6883–6889

Parsek MR, Fuqua C (2004) Biofilms 2003: emerging themes and challenges in studies of surface-associated microbial life. J Bacteriol 186:4427–4440

Salerno MB, Logan BE, Velegol D (2004) Importance of molecular details in predicting bacterial adhesion to hydrophobic surfaces. Langmuir 20:10625–10629

September SM, Els FA, Venter SN, Brozel VS (2007) Prevalence of bacterial pathogens in biofilms of drinking water distribution systems. J Water Health 5:219–227

Sheng XX, Ting YP, Pehkonen SO (2007) Force measurements of bacterial adhesion on metals using a cell probe atomic force microscope. J Colloid Interface Sci 310:661–669

Simpson DR (2008) Biofilm processes in biologically active carbon water purification. Water Res 42:2839–2848

Singh R, Paul D, Jain RK (2006) Biofilms: implications in bioremediation. Trends Microbiol 14:389–397

Sykes ECH, Tikhov MS, Lambert RM (2002) Surface composition, morphology, and catalytic activity of model polycrystalline Titania surfaces. J Phys Chem B 106:7290–7294

Szewzyk U, Szewzyk R, Manz W, Schleifer KH (2000) Microbiological safety of drinking water. Annu Rev Microbiol 54:81–127

Vadillo-Rodriguez V, Logan BE (2006) Localized attraction correlates with bacterial adhesion to glass and metal oxide substrata. Environ Sci Technol 40:2983–2988

van Loosdrecht MCM, Lyklema J, Norde W, Zehnder AJB (1989) Bacterial adhesion—a physicochemical approach. Microb Ecol 17:1–15

Wenzler LA, Moyes GL, Beebe TP (1996) Improvements to atomic force microscopy cantilevers for increased stability. Rev Sci Instrum 67:4191–4197